UAV-Assisted Physical Layer Security in Multi-Beam Satellite-Enabled Vehicle Communications

Zhisheng Yin, *Member, IEEE*, Min Jia, *Senior Member, IEEE*, Nan Cheng, *Member, IEEE*, Wei Wang, *Member, IEEE*, Feng Lyu, *Member, IEEE*, Qing Guo, *Member, IEEE*, and Xuemin Shen, *Fellow, IEEE*

***Abstract*— In this paper, we investigate unmanned aerial vehicle (UAV) assisted physical layer security in multi-beam satellite enabled vehicle communications. Particularly, the UAV is exploited as a relay to improve the secure satellite-to-vehicle link, and simultaneously serves as a jammer by deliberately generating artificial noise (AN) to confuse Eve. The satellite beamforming (BF) and UAV power allocation (PA) are jointly optimized to maximize the secrecy rate of the legitimate user within a target beam while guaranteeing the quality of service (QoS) of users within other beams. Since the problem is nonconvex, we first convert it into an equivalent two-stage problem. Then, the outer-stage problem is solved by using one-dimensional search, and the inner-stage problem is transformed to a bi-convex problem by using the semi-definite relaxation (SDR) and Charnes Cooper transformation. To solve the inner-stage bi-convex problem, we propose an iterative alternating optimization algorithm, where the optimal BF is obtained by semi-definite programming (SDP), and the optimal UAV PA is subsequently obtained by solving the reformulated fractional programming problem with an iterative Dinkelbach method. The tightness of SDR and the complexity of our proposed approach are analyzed, and extensive simulations are carried out to evaluate the effectiveness of our proposed approach.**

***Index Terms*— Satellite-enabled vehicle communications, UAV relay, channel similarity, physical layer security.**

Manuscript received December 22, 2020; revised April 18, 2021; accepted May 28, 2021. Date of publication June 23, 2021; date of current version March 9, 2022. This work was supported in part by the National Natural Science Foundation of China under Grant 62071356 and Grant 62002389, in part by the Natural Science Foundation of Jiangsu Province under Grant BK20200440, in part by the Fundamental Research Funds for the Central Universities under Grant NT2020009, and in part by the Natural Sciences and Engineering Research Council (NSERC) of Canada. The Associate Editor for this article was N. Zhang. *(Corresponding author: Nan Cheng.)*

Zhisheng Yin and Nan Cheng are with the State Key Laboratory of ISN, Xidian University, Xi'an 710071, China, and also with the School of Cyber Engineering, Xidian University, Xi'an 710071, China (e-mail: zsyin@xidian.edu.cn; dr.nan.cheng@ieee.org).

Min Jia and Qing Guo are with the School of Electronics and Information Engineering, Harbin Institute of Technology, Harbin 150008, China (e-mail: jiamin@hit.edu.cn; qguo@hit.edu.cn).

Wei Wang is with the College of Electronic Information Engineering, Nanjing University of Aeronautics and Astronautics, Nanjing 211106, China (e-mail: wei_wang@nuaa.edu.cn).

Feng Lyu is with the School of Computer Science and Engineering, Central South University, Changsha 410083, China (e-mail: fenglyu@csu.edu.cn).

Xuemin Shen is with the Department of Electrical and Computer Engineering, University of Waterloo, Waterloo, ON N2L 3G1, Canada (e-mail: sshen@uwaterloo.ca).

Digital Object Identifier 10.1109/TITS.2021.3090017

I. Introduction

SPACE-AIR-GROUND integrated network (SAGIN) enables full network coverage range and flexible resource management, which can increase the network capability, provides seamless connectivity, and enhance network performance [1]. Recently, researchers have actively engaged in investigating the application prospects and technical challenges of SAGIN in vehicular communication networks [2]–[4]. As an irreplaceable part in the next-generation Intelligent Transportation Systems (ITSs), vehicular communication networks enable vehicles to exchange information with other vehicles and the external environments [5], [6]. Due to the limitation of deployment and coverage, it remains inefficient ITSs in remote areas with insufficient terrestrial network infrastructures [7], [8]. With the advantage of coverage, SAGIN can provide the seamless user experience and always-on connectivity for ITSs. However, due to the inherent broadcasting nature and broad coverage, the satellite downlinks in SAGIN-enabled vehicle communications are vulnerable to security threats [9], [10]. Particularly, the attackers and eavesdroppers (Eves) within satellite coverage are difficult to be eliminated as they are able to hide in very large and complex geographical areas, resulting in serious security issues [11].

Different from the upper-layer security approaches, physical layer security can achieve secure transmission by exploiting the intrinsic randomness of wireless channels, which has been potentially investigated in terrestrial wireless communications and vehicular networks [12]–[14]. In order to improve the secrecy performance, several related works have shown that the terrestrial resource can be utilized to assist the physical layer security in satellite communications [15]–[17]. Particularly, by beamforming (BF) at the base station (BS), the green interference served by BS can be leveraged to unequally damage the main and eavesdropping channels of satellite users. However, this idea becomes invalid in areas where only satellite beam exists without the terrestrial network coverage. Considering the inter-beam/co-channel interference caused by frequency reuse among satellite beams, the satellite BF approaches have been leveraged to eliminate the co-channel interference or null useful signals to Eve [18]. However,

satellite spot beams are not narrow enough to distinguish between the legitimate user and Eve, and thus the conventional BF approaches lose efficiency when the channel difference between the legitimate user and Eve becomes negligible. Besides, relaying for satellite-ground secure transmissions generally only focus on the relaying links without considering information leakage in the direct satellite-ground link [19].

In this paper, we consider the secure transmission in downlink multi-beam satellite-enabled vehicle communications within areas in shortage of terrestrial network coverage. Specifically, one Eve is considered to wiretap an interested legitimate user in a specific beam. Considering the distance difference from satellite to the legitimate user and Eve is negligible, the main and wiretap channels are similar with weak random difference, posing challenges in implementing physical layer security techniques [20]. To improve the secrecy rate performance of the legitimate user, we exploit an unmanned aerial vehicle (UAV) to enhance the random difference between the main and wiretap channels. Based on this framework, we then maximize the secrecy rate of the legitimate user within a target beam with ensuring the quality of service (QoS) of users within other beams. The main contributions of this paper are as follows.

- We propose a framework to conduct physical layer security for the downlink multi-beam satellite-enabled vehicle communications, where full frequency reuse is adopted among beams and the inter-beam/co-channel interference is non-negligible. In order to enhance the secure transmission in the downlink multi-beam satellite-enabled vehicle communications, we exploit an UAV to cooperate with the satellite-vehicle link by adopting amplify and forward (AF) with fixed BF scheme (maximum ratio transmission (MRT)/zero-forcing (ZF)). Moreover, we consider a worst case that the Eve is under the UAV coverage and artificial noise (AN) is created by the UAV to confuse the Eve.
- Considering the power constraints of both satellite and UAV, we formulate a problem to maximize the secrecy rate of satellite-vehicle link by jointly optimizing the BF of multi-beam satellite and the power allocation (PA) of UAV for AF and AN. In addition, the predefined QoS, i.e., minimum data rate, for users in other beams within the co-channel of the legitimate user is simultaneously satisfied. To solve the nonconvex problem, we first transfer it to an equivalent two-stage problem. In the outer stage, a single-variable optimization problem is achieved, which is then solved by the one-dimensional search. For the inner-stage problem, the semi-definite relaxation (SDR) and the Charnes-Cooper transformation are used to reformulate it as a bi-convex problem. Moreover, the tightness of rank-one relaxation is proved.
- To solve the bi-convex problem in the inner stage, we propose an iterative alternating optimization approach. Specifically, a semi-definite programming (SDP) approach is used to optimize the BF of multi-beam satellite, and then a fractional programming problem is derived to optimize the UAV PA, which is solved by the iterative Dinkelbach's method. In addition, the complexity of the proposed approach is analyzed, and extensive numerical results are carried out to verify the effectiveness of our proposed approach.

The remainder of this paper is organized as follows. In Section II, the related works are investigated. In Section III, we first present the system model of UAV-assisted secure multi-beam satellite downlink communications, and then formulate a constrained optimization problem to maximize the secrecy rate in Section IV. In Section V, we jointly optimize the satellite BF and UAV PA to solve the nonconvex problem. In Section VI, simulations are carried out to evaluate the secrecy rate performance. Finally, we conclude this paper and direct our future work in Section VII.

Notations: $(\cdot)^T$ and $(\cdot)^\dagger$ denote the transpose and Hermitian transpose, respectively. $|\cdot|$ and $\|\cdot\|$ stand for the absolute value and Euclidean norm of a vector. $\mathrm{Tr}\,(\cdot)$ and $\mathrm{Rank}\,(\cdot)$ denote the trace and rank of a matrix, respectively. $\mathbb{C}^{N\times M}$ denotes a complex space of $N \times M$. $\mathcal{N}\left(\mu, \delta^2\right)$ and $\mathcal{CN}(\mu, \delta^2)$ denote the normal and complex Gaussian distribution with mean μ and variance δ^2, respectively. $\odot$ is the Hadamard product.

II. Related Works

In this section, we review the state-of-the-art physical layer security in satellite-terrestrial communications. Considering satellite coexists with terrestrial networks and shares the spectrum resource, the resources of terrestrial BSs, i.e., multiple antennas and power, are leveraged to assist satellite links to conduct secure transmissions [15]–[17], [21]. Particularly, the BS serves as a green interference resource to combat the malicious eavesdropping attack [15]. Based on the hybrid and partial ZF-based BF at BS, the secrecy performance of satellite links is analyzed in [21], where the interference from BS to satellite user is suppressed by the proposed BF scheme, while Eve is degraded by the interference. In addition, an improved secrecy rate is achieved through optimizing the BF at BS with minimizing the transmit power in [15]. Considering satellite carries multi-antenna, joint BF of satellite and BS is proposed to achieve the positive secrecy rate of satellite-terrestrial links [16]. To improve the secrecy rate of satellite user, a cooperative BF scheme at satellite and BS is proposed to increase the signal-to-interference-plus-noise ratio (SINR) of legitimate satellite user and decrease the SINR of Eve in [17], where BS performs as a friendly jammer to minimize the interference from BS to legitimate satellite user and confuse Eve. The aforementioned works have well investigated secure transmissions in satellite-terrestrial links with the assistance of terrestrial BS. However, they rely much on the terrestrial resource and only one satellite beam is considered.

In multi-beam satellite communications, the partial and full frequency reuse schemes are two typical categories for multi-beam satellite service, and higher spectral efficiency can be achieved by a more aggressive frequency reuse factor along with interference mitigation techniques [22], [23]. Indeed, the inter-beam/co-channel interference caused by spectral sharing is typically considered undesirable, which limits the overall system performance [23], [24]. However, by careful BF design with multi-beam antenna, the inter-beam interference (IBI) can

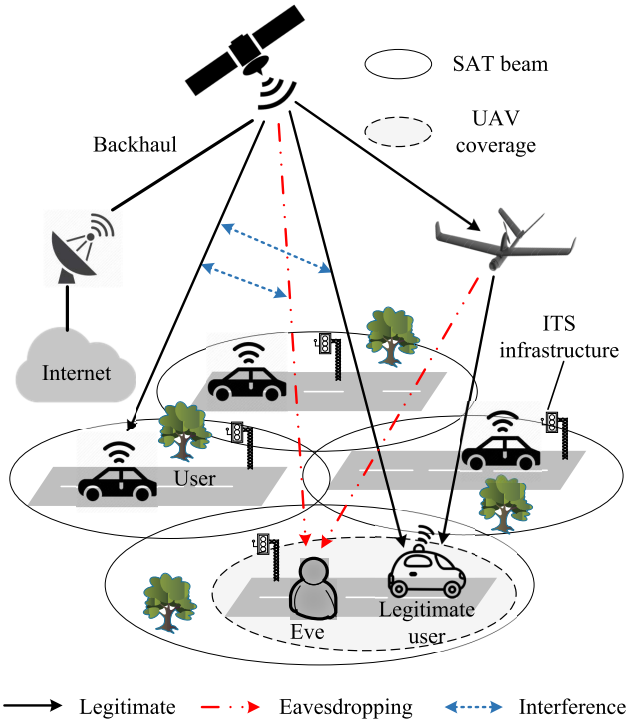

Fig. 1. UAV-assisted secure transmission in multi-beam satellite-enabled vehicle communications.

be beneficial for the physical layer security. Several related works on the secure transmission in multi-beam satellite communications are conducted. A partial ZF-based BF approach is proposed to only null useful signals to Eve and minimize the satellite transmission power [25]. Considering the secrecy rate in each beam with satellite transmit power constraint, a problem to maximize the minimal secrecy rate of multi-beam is studied by optimizing the satellite BF in [18]. However, the aforementioned works are associated with BF design at satellite and without considering the channel similarity between satellite-terrestrial links. The satellite spot beams are not narrow enough to distinguish between the legitimate user and Eve when the Eve hides very near the legitimate user.

III. System Model

As shown in Fig. 1, we consider a multi-beam satellite-enabled vehicle communication system where N beams are formed by adopting the single feed per beam (SFPB) architecture [26]. Full frequency is reused among all the beams and frequency division multiple access (FDMA) is employed for the downlink from satellite to vehicles in each beam [27]. Without loss of generality, we only consider one sub-channel in each beam, and only one vehicle exists in the sub-channel as the satellite user (SU). Particularly, we consider one Eve in a specific beam targeting to wiretap the legitimate user who works at the same sub-channel within the same beam. Meanwhile, the QoS requirement of SUs operating in the same sub-channel of other beams should be ensured. We assume that both SUs and Eve are equipped with a single receive antenna. To improve the secrecy rate from satellite to the legitimate user, UAV as an on-demand relay is deployed to enhance the main channel and serves as a jammer to degrade the eavesdropping channel by sending AN. In addition, the UAV is equipped with a single receive antenna and M transmit antennas. The channel state information (CSI) of SUs and Eve are known at UAV.[1] The main notations and definitions are demonstrated in Table I.

TABLE I
Main Notations and Definitions

Notation	Definition
N	number of satellite beams
M	number of UAV transmit antennas
SU_i	user in the i^{th} beam (legitimate user)
$\mathbf{h}_{sd} \in \mathbb{C}^{N\times 1}$	channel vector from satellite to the legitimate user
$\mathbf{h}_{sr} \in \mathbb{C}^{N\times 1}$	channel vector from satellite to UAV
$\mathbf{h}_{se} \in \mathbb{C}^{N\times 1}$	channel vector from satellite to Eve
$\mathbf{h}_{rd} \in \mathbb{C}^{M\times 1}$	channel vector from UAV to the legitimate user
$\mathbf{h}_{re} \in \mathbb{C}^{M\times 1}$	channel vector from UAV to Eve
$\mathbf{w}_n \in \mathbb{C}^{N\times 1}$	satellite BF vector for the n^{th} beam
$\mathbf{f} \in \mathbb{C}^{M\times 1}$	UAV downlink BF vector
$\mathbf{v} \in \mathbb{C}^{(M-1)\times 1}$	AN vector
ϕ	PA coefficient for the AF signal
U_h	UAV altitude

A. Channel Model

1) Satellite-to-Ground Channel: The channels from satellite to SUs experience the free space path loss (FSPL) and rain attenuation, where the FSPL coefficient is defined by [29]

$$\mathrm{C}_L = \left(\frac{\lambda_w}{4\pi}\right)^2 \frac{1}{d_0^2 + d_h^2}, \tag{1}$$

where λ_w denotes the signal wavelength, d_0 denotes the distance between centers of the beam and satellite coverage, and d_h denotes the height of satellite. The rain attenuation is the dominant factor among atmospheric effects, which depends on the location of the receiver, the frequency of operation, polarization and the elevation angle toward satellite. According to ITU-R P.618 [29], the channel gain caused by rain attenuation can be modeled as a log-normal random variable, i.e., $\ln(\zeta_{dB}) \sim \mathcal{N}(\mu_{\zeta_{dB}}, \delta^2)$, where $\mu_{\zeta_{dB}}$ and δ^2 denote the log-normal location and scale parameter, respectively, and ζ_{dB} is the channel gain in dB. The rain attenuation fading vector of the satellite-to-ground channel can be expressed as

$$\tilde{\mathbf{h}} = \zeta^{-\frac{1}{2}} \exp(-j\boldsymbol{\theta}), \tag{2}$$

where $\boldsymbol{\theta} \in \mathbb{C}^{N\times 1}$ is the phase vector with each component uniformly distributed over $[0, 2\pi)$.

[1]Similar to most of the related works, such as [16] and [28], we assume perfect CSIs of SUs and Eve are known at UAV.

Besides, the beam gain is determined by the satellite antenna pattern and the position of destinations, where the gain for the SU_i is given by [29]

$$b_i\left(\alpha_i\right) = G_i\left(\frac{J_1\left(u_i\right)}{2u_i} + 36\frac{J_3\left(u_i\right)}{u_i^2}\right)^2, \tag{3}$$

with $u_i = 2.07123\frac{\sin(\alpha_i)}{\sin\left(\alpha_{i,3\mathrm{dB}}\right)}$, where G_i is the maximum satellite antenna gain for the i^{th} beam, α_i represenets the elevation angle between SU_i and the center of i^{th} beam, and $\alpha_{i,3\mathrm{dB}}$ is the 3 dB angle of the i^{th} beam. Additionally, $J_1(\cdot)$ and $J_3(\cdot)$ are the first-kind Bessel functions of order 1 and 3, respectively.

Based on the above considerations, the channel vector from satellite to SU_i can be formulated as

$$\mathbf{h}_{sd} = \sqrt{C_L}\tilde{\mathbf{h}} \odot \mathbf{b}^{1/2}, \tag{4}$$

where $\mathbf{b} = [b_1, \ldots, b_i, \ldots, b_N]^T$.

2) Air-to-Ground Channel: The air-to-ground transmission experiences both path loss and small-scale fading [30]. The channel power gain from UAV to the destination is given by

$$G_L = \frac{g_0}{U_d^2 + U_h^2}, \tag{5}$$

where g_0 denotes the channel power gain at a reference distance of 1 m, U_d denotes the horizontal distance from UAV to the destination, and U_h is the UAV altitude. As for the small-scale fading, Rician fading model is adopted. Therefore, the air-to-ground channel is represented as

$$\mathbf{h}_{rd} = \sqrt{G_L}\left(\sqrt{\frac{K}{K+1}}\tilde{\mathbf{h}}_{\mathrm{LoS}} + \sqrt{\frac{1}{K+1}}\tilde{\mathbf{h}}_{\mathrm{Ray}}\right), \tag{6}$$

where K is the Rician factor (in dB, i.e., $K_B = 10log_{10}(K)$), $\tilde{\mathbf{h}}_{\mathrm{LoS}} \in \mathbb{C}^{M\times 1}$ denotes the line-of-sight (LoS) component, and $\tilde{\mathbf{h}}_{\mathrm{Ray}} \in \mathbb{C}^{M\times 1}$ represents the non-line-of-sight (NLoS) Rayleigh fading component.

B. Signal Model

The transmitted signal vector by multi-beam satellite is given by

$$\mathbf{x}_s = \sum_{n=1}^{N}\mathbf{w}_n s_n, \tag{7}$$

where $\mathbf{w}_n \in \mathbb{C}^{N\times 1}$ denotes the BF vector for the n^{th} beam and s_n is the intended signal for SU_n with $\mathbb{E}\{|s_n|^2\} = 1$.

Without loss of generality, the satellite user (SU) in the i^{th} beam is assumed to be the targeted user, denoted by SU_i. The UAV is deployed to assist secure transmission from satellite to the legitimate user SU_i, and it works in full-duplex mode.[2] Particularly, the UAV hovers above SU_i to receive the satellite signal and communicates with SU_i simultaneously. The received signal at UAV can be expressed as

$$\begin{aligned} r &= \mathbf{h}_{sr}^{\dagger}\mathbf{x}_s + \nu + n_r \\ &= \mathbf{h}_{sr}^{\dagger}\mathbf{w}_i s_i + \sum_{n\neq i}\mathbf{h}_{sr}^{\dagger}\mathbf{w}_n s_n + \nu + n_r, \end{aligned} \tag{8}$$

where ν denotes the residual self-interference (after self-interference cancellation) with $\nu \sim \mathcal{CN}(0, \sigma_\nu^2)$ [33], and n_r denotes the noise received by UAV with $n_r \sim \mathcal{CN}(0, \sigma_r^2)$. For the UAV downlink, AF is adopted to cooperate with the SU_i, and meanwhile AN is superimposed to confuse the decoding of Eve. Thus, the transmitted signal by UAV is represented as

$$\mathbf{x}_u = \sqrt{\phi P_v}\mathbf{f}\alpha r + \sqrt{(1-\phi)\,P_v}\mathbf{G}\mathbf{v}, \tag{9}$$

where P_v is the transmit power of UAV, ϕ $(0 \le \phi \le 1)$ is the PA coefficient for the AF signal, α is the power scaling factor, and $\mathbf{f} \in \mathbb{C}^{M\times 1}$ denotes the BF vector of UAV and $\|\mathbf{f}\|^2 = 1$, which adopts fixed BF mode in this work. Besides, $\mathbf{v} \in \mathbb{C}^{(M-1)\times 1}$ is an AN vector with i.i.d elements, i.e., $v_i \sim \mathcal{CN}(0, 1/M)$, and $\mathbf{G} \in \mathbb{C}^{M\times(M-1)}$ is designed as a projection matrix into the null of legitimate channel [34], i.e., $\mathbf{G} = \left(\mathbf{I}_M - \mathbf{h}_{rd}\left(\mathbf{h}_{rd}^{\dagger}\mathbf{h}_{rd}\right)^{-1}\mathbf{h}_{rd}^{\dagger}\right)\mathbf{h}_{re}$ with $\mathbf{h}_{rd}^{\dagger}\mathbf{G} = \mathbf{0}$.

Different from related works in relaying for satellite-terrestrial transmissions where the direct link is generally neglected [19], [35], we assume that the direct satellite-vehicle link and UAV cooperative link arrive simultaneously [33]. Thus, the signal received by SU_i is

$$\begin{aligned} y_d &= \mathbf{h}_{sd}^{\dagger}\mathbf{x}_s + \mathbf{h}_{rd}^{\dagger}\mathbf{x}_u + n_d \\ &= \mathbf{a}\mathbf{w}_i s_i + \sum_{n\neq i}\mathbf{a}\mathbf{w}_n s_n + \alpha\sqrt{\phi P_v}\mathbf{h}_{rd}^{\dagger}\mathbf{f}\left(\nu + n_r\right) + n_d, \end{aligned} \tag{10}$$

where $\mathbf{a} = \mathbf{h}_{sd}^{\dagger} + \alpha\sqrt{\phi P_v}\mathbf{h}_{rd}^{\dagger}\mathbf{f}\mathbf{h}_{sr}^{\dagger}$, and n_d denotes the received noise by SU_i with $n_d \sim \mathcal{CN}(0, \sigma_d^2)$. In (10), the first and second terms are the respective expected signal and co-channel interference caused by frequency reuse among beams, and the third term is the amplified self-interference.

For the Eve targeting to wiretap SU_i, we consider a worst case that it hides in the coverage of UAV and wiretaps the direct and cooperative links simultaneously. Similar to (10), the signal received by Eve can be expressed as

$$\begin{aligned} y_e &= \mathbf{h}_{se}^{\dagger}\mathbf{x}_s + \mathbf{h}_{re}^{\dagger}\mathbf{x}_u + n_e \\ &= \mathbf{b}\mathbf{w}_i s_i + \sum_{n\neq i}\mathbf{b}\mathbf{w}_n s_n + \alpha\sqrt{\phi P_v}\mathbf{h}_{re}^{\dagger}\mathbf{f}\left(\nu + n_r\right) \\ &\quad + \sqrt{(1-\phi)\,P_v}\mathbf{h}_{re}^{\dagger}\mathbf{G}\mathbf{v} + n_e, \end{aligned} \tag{11}$$

where $\mathbf{b} = \mathbf{h}_{se}^{\dagger} + \alpha\sqrt{\phi P_v}\mathbf{h}_{re}^{\dagger}\mathbf{f}\mathbf{h}_{sr}^{\dagger}$, and n_e is the received noise with $n_e \sim \mathcal{CN}(0, \sigma_e^2)$.

IV. Problem Formulation

Based on (10), the achievable SINR of SU_i can be expressed as

$$\gamma_d = \frac{|\mathbf{a}\mathbf{w}_i|^2}{\underbrace{\sum_{n\neq i}|\mathbf{a}\mathbf{w}_n|^2}_{\mathrm{IBI}} + \underbrace{\alpha^2\phi P_v\left|\mathbf{h}_{rd}^{\dagger}\mathbf{f}\right|^2\left(\delta_\nu^2 + \delta_r^2\right)}_{\text{AF interference and noise}} + \delta_d^2}, \tag{12}$$

and that of Eve can be obtained similarly by (13), shown at the bottom of the next page, where the IBI is received

[2]UAV-enabled full-duplex relaying communications have been well studied [31], [32], where UAV forwards and receives signals simultaneously.

from satellite and UAV simultaneously, the AF interference and noise are received from the UAV AF link, and AN is received from UAV. Thus, the secrecy rate of SU_i can be calculated as

$$R_s = \left[\log_2(1+\gamma_d) - \log_2(1+\gamma_e)\right]^+, \tag{14}$$

where $[x]^+ = \max(x, 0)$.

In the $j^{th}(j \neq i)$ beam, SU_j only receives the satellite signal, and the achievable rate of SU_j can be obtained as

$$R_j = \log_2\left(1 + \frac{\left|\mathbf{h}_j^\dagger \mathbf{w}_j\right|^2}{\sum\limits_{n\neq j}\left|\mathbf{h}_j^\dagger \mathbf{w}_n\right|^2 + \sigma_j^2}\right), \quad j \neq i, \tag{15}$$

where $\mathbf{h}_j$ denotes the channel vector from satellite to SU_j.

To maximize the secrecy rate of SU_i and guarantee the QoS requirement of SU_j $(j \neq i)$, we jointly optimize the BF vectors of satellite and the PA of UAV. The optimization problem can be formulated as

$$\begin{aligned}
\mathcal{P}1: \quad & \max_{\{\mathbf{w}_n\}_{n=1}^N, \phi} \quad R_s && \text{(16a)}\\
& s.t. \quad R_j \geq Q_j, \quad j \neq i, && \text{(16b)}\\
& \sum_{n=1}^{N} \|\mathbf{w}_n\|^2 \leq P_s, && \text{(16c)}\\
& 0 \leq \phi \leq 1, && \text{(16d)}
\end{aligned}$$

where (16b) is the QoS constraint for SU_j $(j \neq i)$; (16c) refers to the satellite power limitation, where P_s is the maximum transmit power of satellite; with UAV transmit power P_v, the PA of UAV is constrained by ϕ in (16d).

Remark 1: For the AF relaying link from UAV to destination, we consider the widely used MRT/ZF-based BF as the fixed BF scheme of UAV downlink transmission, where the MRT/ZF-based BF vector can be respectively given by

$$\mathbf{f}_{MRT} = \mathbf{h}_{rd} \big/ \|\mathbf{h}_{rd}\|, \tag{17}$$

$$\mathbf{f}_{ZF} = \mathbf{f}_0 \big/ \|\mathbf{f}_0\|, \tag{18}$$

with $\mathbf{f}_0 = \left(\mathbf{I}_M - \mathbf{h}_{re}\left(\mathbf{h}_{re}^\dagger \mathbf{h}_{re}\right)^{-1}\mathbf{h}_{re}^\dagger\right)\mathbf{h}_{rd}$.

Particularly, since the ZF-based BF scheme can null the useful signals from UAV to Eve, i.e., $\mathbf{h}_{re}^\dagger \mathbf{f}_0 = 0$*, UAV only works as the AF relaying but not generates AN and then* $\phi = 1$ *in this case. Thus, it only optimizes satellite BF in* $\mathcal{P}1$ *when the ZF-based BF is adopted by UAV downlink.*

Regardless of the special case with ZF-based BF at UAV, UAV PA coefficient ϕ is optimized in $\mathcal{P}1$, i.e., MRT-based BF. Nevertheless, the problem $\mathcal{P}1$ is highly intractable as it has the nonconvex objective function and constraints. To solve such nonconvex optimization problem, a two-stage optimization approach is proposed in the following section. To facilitate the analysis, we assume that the noise power is normalized, i.e., $\sigma_r^2 = \sigma_d^2 = \sigma_e^2 = 1$ and define $\delta_v^2 \big/ \delta_{sr}^2 = \beta$ to characterize the residual self-interference level of UAV transceiver in the following sections.

V. Joint Satellite BF and UAV PA Optimization

In this section, we first transform the primal problem $\mathcal{P}1$ to a two-stage problem. For the outer-stage problem, it can be solved by one-dimensional search. In the inner stage, a bi-convex optimization problem is obtained through SDR and Charnes-Cooper transformation, which is then solved by our proposed iterative alternating optimization approach. The tightness of SDR and the complexity of the two-stage optimization are also analyzed.

To simplify the objective function of P1, we first introduce a slack variable τ to reformulate P1 as

$$\begin{aligned}
\mathcal{P}2: \quad & \max_{\tau, \{\mathbf{w}_n\}_{n=1}^N, \phi} \quad \log_2(1+\gamma_d) - \log_2\left(\frac{1}{\tau}\right) && \text{(19a)}\\
& s.t. \quad \log_2(1+\gamma_e) \leq \log_2\left(\frac{1}{\tau}\right), && \text{(19b)}\\
& \quad (16b) - (16d) \quad satisfied. && \text{(19c)}
\end{aligned}$$

To determine the feasible domain of τ, a Lemma is introduced as follows.

Lemma 1: Based on (19a) and (19b), the feasible domain of τ *is determined by*

$$\tau_{\min} \triangleq \frac{1}{1 + P_s\left|\mathbf{h}_{sd}^\dagger\right|^2 + \alpha^2 P_s P_v \left|\mathbf{h}_{rd}^\dagger \mathbf{f} \mathbf{h}_{sr}^\dagger\right|^2} \leq \tau \leq 1. \tag{20}$$

$$\gamma_e = \frac{|\mathbf{b}\mathbf{w}_i|^2}{\underbrace{\sum\limits_{n\neq i}|\mathbf{b}\mathbf{w}_n|^2}_{\text{IBI}} + \underbrace{\alpha^2\phi P_v\left|\mathbf{h}_{re}^\dagger \mathbf{f}\right|^2\left(\delta_v^2 + \delta_r^2\right)}_{\text{AF interference and noise}} + \underbrace{(1-\phi)\,P_v\left|\mathbf{h}_{re}^\dagger \mathbf{G}\mathbf{v}\right|^2}_{\text{AN}} + \delta_e^2}. \tag{13}$$

$$\begin{aligned}
\mathcal{P}4: \quad \varphi(\tau) \triangleq & \max_{\{\mathbf{w}_n\}_{n=1}^N, \phi} \quad \tau \frac{\mathbf{w}_i^\dagger \mathbf{a}^\dagger \mathbf{a} \mathbf{w}_i}{\sum\limits_{n\neq i}\mathbf{w}_n^\dagger \mathbf{a}^\dagger \mathbf{a}\mathbf{w}_n + \alpha^2\phi P_v \mathbf{f}^\dagger \mathbf{h}_{rd}\mathbf{h}_{rd}^\dagger \mathbf{f}\,(\beta+1) + 1} && \text{(22a)}\\
& s.t. \quad \frac{\mathbf{w}_i^\dagger \mathbf{b}^\dagger \mathbf{b}\mathbf{w}_i}{\sum\limits_{n\neq i}\mathbf{w}_n^\dagger \mathbf{b}^\dagger \mathbf{b}\mathbf{w}_n + \alpha^2\phi P_v \mathbf{f}^\dagger \mathbf{h}_{re}\mathbf{h}_{re}^\dagger \mathbf{f}\,(\beta+1) + (1-\phi)\,P_v \mathbf{v}^\dagger \mathbf{G}^\dagger \mathbf{h}_{re}\mathbf{h}_{re}^\dagger \mathbf{G}\mathbf{v} + 1} \leq \frac{1}{\tau} - 1, && \text{(22b)}\\
& \quad (16b) - (16d) \quad satisfied. && \text{(22c)}
\end{aligned}$$

Proof: The proof is concluded in Appendix A. ■

From (19a), the objective function can be rewritten as $\log_2(\tau + \tau\gamma_d)$. We then define $\varphi(\tau)$ as the maximum value of $\tau\gamma_d$ satisfying (19b–19c) when τ is fixed. Thus, $\mathcal{P}2$ can be transformed to a two-stage problem, where the outer-stage problem is formulated as

$$\mathcal{P}3: \quad \max_{\tau} \quad \log_2(\tau + \varphi(\tau)) \tag{21a}$$

$$s.t. \quad \tau_{\min} \le \tau \le 1. \tag{21b}$$

To optimize the signal-variable τ in $\mathcal{P}3$, the one-dimensional search method is used where $\varphi(\tau)$ can be evaluated for any feasible τ in the inner stage [36]. However, to this end, the key is to obtain $\varphi(\tau)$. The inner-stage problem to obtain $\varphi(\tau)$ is formulated as $\mathcal{P}4$ in (22), shown at the bottom of previous page. We can see that $\mathcal{P}4$ is still intractable, due to obstacles from the quadratic fractional form in the objective function and the nonconvex constraints.

A. SDR and Charnes-Cooper Transformation

To overcome the quadratic forms in $\mathcal{P}4$, we replace the optimization variables by $\mathbf{W}_n = \mathbf{w}_n\mathbf{w}_n^\dagger$ with $n = 1, \ldots, N$, and adopt SDR to ignore the rank-one constraint of $\mathbf{W}_n$. In addition, we make some definitions for transformation, such as, $\mathbf{A} = \mathbf{a}^\dagger\mathbf{a}$, $\mathbf{B} = \mathbf{b}^\dagger\mathbf{b}$, $\mathbf{F} = \mathbf{f}\mathbf{f}^\dagger$, $\mathbf{H}_{rd} = \mathbf{h}_{rd}\mathbf{h}_{rd}^\dagger$, $\mathbf{H}_{re} = \mathbf{h}_{re}\mathbf{h}_{re}^\dagger$, and $\mathbf{H}_j = \mathbf{h}_j\mathbf{h}_j^\dagger$. Thus, $\mathcal{P}4$ can be relaxed as

$$\mathcal{P}5: \max_{\{\mathbf{W}_n\}_{n=1}^N, \phi} \tau \frac{\mathrm{Tr}(\mathbf{A}\mathbf{W}_i)}{\sum_{n\neq i}\mathrm{Tr}(\mathbf{A}\mathbf{W}_n) + \psi_d\phi + 1} \tag{23a}$$

$$s.t. \ \frac{\mathrm{Tr}(\mathbf{B}\mathbf{W}_i)}{\sum_{n\neq i}\mathrm{Tr}(\mathbf{B}\mathbf{W}_n) + p_v\mathrm{Tr}(\mathbf{H}_{re}\mathbf{C}) + \psi_e\phi + 1} \le \frac{1}{\tau} - 1, \tag{23b}$$

$$\frac{\mathrm{Tr}(\mathbf{H}_j\mathbf{W}_j)}{\mathrm{Tr}(\sum_{n\neq j}\mathbf{H}_j\mathbf{W}_n) + 1} \ge \varepsilon_j, \quad j \neq i, \tag{23c}$$

$$\sum_{n=1}^{N}\mathrm{Tr}(\mathbf{W}_n) \le P_s, \tag{23d}$$

$$\mathbf{W}_n \succeq \mathbf{0}, \quad n = 1, \ldots, N, \tag{23e}$$

$$0 \le \phi \le 1, \tag{23f}$$

where $\psi_d = \alpha^2 p_v(\beta+1)\mathrm{Tr}(\mathbf{H}_{rd}\mathbf{F})$, $\mathbf{C} = \mathbf{G}\mathbf{v}\mathbf{v}^\dagger\mathbf{G}^\dagger$, $\psi_e = p_v\mathrm{Tr}\left(\mathbf{H}_{re}\left(\alpha^2(\beta+1)\mathbf{F} - \mathbf{C}\right)\right)$, and $\varepsilon_j = 2^{Q_j} - 1$. Particularly, the constraints (23c)–(23f) correspond to (16b)–(16d), respectively, where the constraints (23b) and (23c) are nonconvex. Let $\xi = \frac{1}{\tau} - 1$, the constraint (23b) can be rewritten as

$$\mathrm{Tr}(\mathbf{B}\mathbf{W}_\Delta) - \xi p_v\mathrm{Tr}(\mathbf{H}_{re}\mathbf{C}) - \xi\psi_e\phi \le \xi, \tag{24}$$

where $\mathbf{W}_\Delta = \mathbf{W}_i - \sum_{n\neq i}\xi\mathbf{W}_n$. The constraint (23c) can be represented as

$$\mathrm{Tr}(\mathbf{H}_j(\mathbf{W}_j - \sum_{n\neq j}\varepsilon_j\mathbf{W}_n)) \ge \varepsilon_j. \tag{25}$$

Moreover, $\mathbf{A}$ and $\mathbf{B}$ are functions of ϕ, which are associated with the UAV PA. Thus, the objective function in (23a) is still nonconvex since the fractional polynomial and the multiplication of multiple variables. To reduce the fractional polynomial, a Charnes-Cooper transformation is adopted by introducing an auxiliary variable, which is given by

$$\eta = \frac{\tau}{\sum_{n\neq i}\mathrm{Tr}(\mathbf{A}\mathbf{W}_n) + \psi_d\phi + 1}. \tag{26}$$

Then, we make the changes of variables for optimizing the satellite BF by $\bar{\mathbf{W}}_n = \eta\mathbf{W}_n (n = 1, \ldots, N)$, and thus the objective function of $\mathcal{P}5$ can be rewritten as $\mathrm{Tr}(\mathbf{A}\bar{\mathbf{W}}_i)$, which is biconvex for optimizing the satellite BF and the UAV PA. To solve such a biconvex problem, an iterative alternating optimization approach is proposed.

B. Iterative Alternating Optimization Approach

In this section, we propose a SDP approach for optimizing the satellite BF when ϕ is fixed. Based on the feasible satellite BF, a fractional programming problem is equivalently reformulated for optimizing the UAV PA, which is solved by the Dinkelbach's method. Then, the alternating optimization can be conducted iteratively.

1) SDP Approach to Obtain Satellite BF: Given a ϕ, $\mathbf{A}$ and $\mathbf{B}$ are fixed. By using (24–26), the problem $\mathcal{P}5$ can be reduced to a convex problem for optimizing the satellite BF with the auxiliary variable of η, which can be reformulated as

$$\mathcal{P}6-\mathrm{A}: \max_{\{\bar{\mathbf{W}}_n\}_{n=1}^N, \eta} \mathrm{Tr}(\mathbf{A}\bar{\mathbf{W}}_i) \tag{27a}$$

$$\text{s.t.} \ \sum_{n\neq i}\mathrm{Tr}(\mathbf{A}\bar{\mathbf{W}}_n) + \eta\psi_d\phi + \eta = \tau, \tag{27b}$$

$$\mathrm{Tr}(\mathbf{B}\bar{\mathbf{W}}_\Delta) - \eta\xi(p_v\mathrm{Tr}(\mathbf{H}_{re}\mathbf{C}) + \psi_e\phi) \le \eta\xi, \tag{27c}$$

$$\mathrm{Tr}(\mathbf{H}_j(\bar{\mathbf{W}}_j - \sum_{n\neq j}\varepsilon_j\bar{\mathbf{W}}_n)) \ge \eta\varepsilon_j, \quad j \neq i, \tag{27d}$$

$$(23d), (23e) \quad satisfied. \tag{27e}$$

It is noteworthy that $\mathcal{P}6$-A is a SDP problem, which can be efficiently solved by CVX tools [37]. Assuming $\bar{\mathbf{W}}_n^\star$ with $n = 1, \ldots, N$ and $\eta^\star$ to be the optimal solutions for $\mathcal{P}6$-A, $\mathbf{W}_n^\star$ can be obtained by $\frac{\bar{\mathbf{W}}_n^\star}{\eta^\star}$, accordingly.

Particularly, given $\phi = 1$ and replacing $\mathbf{f}$ with $\mathbf{f}_{ZF}$, the optimal satellite BF can be obtained by solving $\mathcal{P}6$-A for maximizing the secrecy rate of SU_i with UAV cooperation AF by adopting the ZF-based BF.

2) Fractional Programming to Optimize UAV PA: For the fixed satellite BF, optimizing the UAV PA in $\mathcal{P}4$ is equivalent to that in $\mathcal{P}5$. By using $\bar{\mathbf{W}}_n^\star$ with $n = 1, \ldots, N$, we equivalently reformulate $\mathcal{P}4$ for optimizing ϕ, which can be expressed as

$$\mathcal{P}6-B: \quad \max_{x} \quad \frac{f(x)}{g(x)} \tag{28a}$$

$$s.t. \quad a_3x^2 + b_3x + c_3 \le 0, \tag{28b}$$

$$0 \le x \le 1, \tag{28c}$$

where $x = \sqrt{\phi}$, $f(x) = a_1x^2 + b_1x + c_1$ and $g(x) = a_2x^2 + b_2x + c_2$ with the coefficients $\{a_1, b_1, c_1\}$, $\{a_2, b_2, c_2\}$, and $\{a_3, b_3, c_3\}$ being constants, which are conducted in (29), shown at the bottom of the page. Particularly, it can be seen that $\mathcal{P}$6-B is a fractional programming problem, which is still nonconvex. Further, we introduce the following Lemma to reformulate it.

Lemma 2: For $f(x) \ge 0, g(x) > 0$, the maximum objective value $q^\star = \frac{f(x^\star)}{g(x^\star)} = \max_x \frac{f(x)}{g(x)}$ can be achieved if and only if $q^\star$ and $x^\star$ satisfy

$$\max_x f(x) - q^\star g(x) = f\left(x^\star\right) - q^\star g\left(x^\star\right) = 0. \tag{30}$$

Proof: The proof can be found in [38]. ∎

According to Lemma 2, $\mathcal{P}$6-B is equivalent to find $q^\star$ and $x^\star$ within a feasible region[3] $\mathcal{D}$ determined by constraints in (28b) and (28c). Specifically, the Dinkelbach's method can be used to solve the problem iteratively [38]. Given an initial $q_0^\star$, the following subproblem should be solved in each iteration,

$$\max_{x\in\mathcal{D}} \Phi_l(x), \tag{31}$$

where $\Phi_l(x) \triangleq f(x) - q_l^\star g(x)$, and $q_l^\star$ is obtained in the previous iteration. It can be seen that the concavity or convexity of $\Phi_l(x)$ is leveraged by

$$\frac{\partial^2 \Phi_l(x)}{\partial x^2} = 2\left(a_1 - q_l{}^\star a_2\right). \tag{32}$$

Based on (32), if $\frac{\partial^2 \Phi_l(x)}{\partial x^2} < 0$ ($a_1 < q_l{}^\star a_2$), $\Phi_l(x)$ is convex and there exists a maximum value, which is achieved by

$$x_l^\circ = \frac{q_l{}^\star b_2 - b_1}{2(a_1 - q_l{}^\star a_2)}), \tag{33}$$

with $\left.\frac{\partial \Phi_l(x)}{\partial x}\right|_{x_l^\circ} = 0$. Particularly, if $x_l^\circ \in \mathcal{D}$, the optimal solution is $x_l^\star = x_l^\circ$. Otherwise, it is given by

$$x_l^\star = \underset{x\in\partial\mathcal{D}}{\operatorname{argmax}}\, \Phi_l(x), \tag{34}$$

where $\partial\mathcal{D}$ denotes the point-set of the boundary of $\mathcal{D}$. If $\frac{\partial^2 \Phi_l(x)}{\partial x^2} \ge 0$ ($a_1 \ge q_l{}^\star a_2$), $\Phi_l(x)$ is concave and the optimal $x_l^\star$ can be obtained based on (34).

[3]Given a_3, b_3, and c_3, the feasible region determined by (28b) can be figured out with using its monotonicity, which is then taken intersection with (28c) to obtain the $\mathcal{D}$.

For the $(l+1)^{th}$ iteration, the q_{l+1} can be updated by

$$q_{l+1}^\star = \frac{f\left(x_l^\star\right)}{g\left(x_l^\star\right)}. \tag{35}$$

Given a convergence tolerance $\epsilon_1 > 0$, the iterative process could be terminated when

$$\left|f\left(x_l^\star\right) - q_l g\left(x_l^\star\right)\right| < \epsilon_1. \tag{36}$$

Moreover, due to the convergence of such a fractional programming [39], the optimal $x^\star$ can be obtained. Finally, the $\mathcal{P}$6-B is solved and the optimal UAV PA is obtained by $\phi^\star = (x^\star)^2$.

Finally, we give the algorithm procedure to find the optimal solutions of satellite BF and UAV PA in Algorithm 1. Particularly, ϵ_0 and ϵ_2 are the convergence tolerances of iterative alternating and one-dimensional search, respectively. However, it is worthing noting that the rank-one constraint has been relaxed by SDR in the transformation from $\mathcal{P}$4 to $\mathcal{P}$5, and $\mathcal{P}$6-A succeeds the relaxation. To confirm the tightness of the relaxation, we prove the rank-one of solutions for $\mathcal{P}$6-A as follows.

C. Tightness Analysis

We consider the following power minimization problem to prove the rank condition of $\mathbf{W}_n^\star$ with $n = 1, \ldots, N$, which is formulated as

$$\mathcal{P}7: \min_{\{\mathbf{W}_n\}_{n=1}^N, \phi} \sum_{n=1}^{N} \mathrm{Tr}(\mathbf{W}_n) \tag{37a}$$

$$s.t. \quad \tau \mathrm{Tr}(\mathbf{A}\mathbf{W}_i) - u^*\Big(\sum_{n\ne i} \mathrm{Tr}(\mathbf{A}\mathbf{W}_n) + \psi_d\phi\Big) \ge u^*, \tag{37b}$$

$$(23d) - (23f), (24), (25) \quad satisfied. \tag{37c}$$

In (37b), μ^* denotes the optimal objective value of problem $\mathcal{P}$5. We first introduce the following Proposition to prove that $\mathcal{P}$7 is equivalent to $\mathcal{P}$5.

Proposition 1: Any feasible solution of $\mathcal{P}$7 is optimal for $\mathcal{P}$5.

Proof: It can be seen that (23b)–(23f) in $\mathcal{P}$5 are all active in $\mathcal{P}$7. Supposing $\left\{\mathbf{W}_n^\circ\right\}_{n=1}^N$ and ϕ° are the feasible solutions to $\mathcal{P}$7, which indeed satisfy $\mathcal{P}$5. Meanwhile, the following

$$\begin{cases} a_1 = \alpha^2 p_v \mathrm{Tr}(\mathbf{H}_{rd}\mathbf{F}\mathbf{H}_{sr}\mathbf{W}_i); & b_1 = \alpha\sqrt{p_v}\mathrm{Tr}\left(\left(\mathbf{h}_{sr}\mathbf{f}^\dagger\mathbf{h}_{rd}\mathbf{h}_{sd}^\dagger + \mathbf{h}_{sd}\mathbf{h}_{rd}^\dagger\mathbf{f}\mathbf{h}_{sr}^\dagger\right)\mathbf{W}_i\right); \\ a_2 = \frac{1}{\tau}\alpha^2 p_v \mathrm{Tr}\left(\mathbf{H}_{rd}\mathbf{F}\mathbf{H}_{sr}\sum_{n\ne i}\mathbf{W}_n\right) + \psi_d; & b_2 = \frac{1}{\tau}\alpha\sqrt{p_v}\mathrm{Tr}\left(\left(\mathbf{h}_{sr}\mathbf{f}^\dagger\mathbf{h}_{rd}\mathbf{h}_{sd}^\dagger + \mathbf{h}_{sd}\mathbf{h}_{rd}^\dagger\mathbf{f}\mathbf{h}_{sr}^\dagger\right)\sum_{n\ne i}\mathbf{W}_n\right); \\ a_3 = \alpha^2 p_v \mathrm{Tr}(\mathbf{H}_{re}\mathbf{F}\mathbf{H}_{sr}\mathbf{W}_\Delta) - \xi\psi_e; & b_3 = \alpha\sqrt{p_v}\mathrm{Tr}\left(\left(\mathbf{h}_{sr}\mathbf{f}^\dagger\mathbf{h}_{re}\mathbf{h}_{se}^\dagger + \mathbf{h}_{se}\mathbf{h}_{re}^\dagger\mathbf{f}\mathbf{h}_{sr}^\dagger\right)\mathbf{W}_\Delta\right); \\ c_1 = \mathrm{Tr}\left(\mathbf{H}_{sd}\mathbf{W}_i\right); c_2 = \frac{1}{\tau}\mathrm{Tr}\left(\mathbf{H}_{sd}\sum_{n\ne i}\mathbf{W}_n\right) + 1; & c_3 = \mathrm{Tr}(\mathbf{H}_{se}\mathbf{W}_\Delta) - \xi p_v \mathrm{Tr}(\mathbf{H}_{re}\mathbf{C}) - \xi. \end{cases} \tag{29}$$

Algorithm 1 Joint Satellite BF and UAV PA Optimization

Input: $\mathbf{f}, \alpha, \beta$.
Result: $\{\{\mathbf{w}_n^\star, n = 1, \ldots, N\}, \phi^\star\}$.
Initialization: ϕ_0, the tolerances ϵ_0, ϵ_1, and ϵ_2.
Set $t = 0$;
repeat
  $\tau^{(t)} = \tau_{min} + \frac{t}{(L-1)}(\tau_{max} - \tau_{min})$.
  while $(|u^\star - q^\star| > \epsilon_0)$ **do**
    Begin SDP with using CVX tool to solve $\mathcal{P}6$-A;
    Output: $\bar{\mathbf{W}}_n^\star$, $\eta^\star$, and the objective value $u^\star$.
    Obtain $\mathbf{W}_n^\star = \frac{\bar{\mathbf{W}}_n^\star}{\eta^\star}$ $(n = 1, \ldots, N)$, and then calculate $\{a_1, b_1, c_1\}$, $\{a_2, b_2, c_2\}$, and $\{a_3, b_3, c_3\}$ based on (29).
    Initialize q_0.
    Set $l = 0$;
    while $\left(\left|f\left(x_l^\star\right) - q_l g\left(x_l^\star\right)\right| > \epsilon_1\right)$ **do**
      Determine $\mathcal{D}$ and obtain $x_l^\circ = \frac{q_l b_2 - b_1}{2(a_1 - q_l a_2)}$;
      if $(a_1 < q_l a_2)$ & $(x_l^\circ \in \mathcal{D})$ **then**
        $x_l^\star = x_l^\circ$;
      else
        $x_l^\star = \underset{x \in \partial\mathcal{D}}{\operatorname{argmax}} \Phi_l(x)$;
      Update $q_{l+1}^\star = \frac{f(x_l^\star)}{g(x_l^\star)}$;
    Output: $\phi^\star = (x^\star)^2$ and the objective value $q^\star$.
    Return $\phi = \phi^\star$ to step 6;
  Output: $\varphi(\tau^{(t)}) = max(u^\star, q^\star)$.
until $\left|\tau^{(t+1)} + \varphi(\tau^{(t+1)}) - \tau^{(t)} - \varphi(\tau^{(t)})\right| < \epsilon_2$;
Obtain $\mathbf{w}_n^\star$ by the singular value decomposition (SVD) of $\mathbf{W}_n^\star$, $n = 1, \ldots, N$.
Procedure End

condition is satisfied based on the constraint (37b)

$$u^* \leq \frac{\tau \mathrm{Tr}\left(\mathbf{A}\mathbf{W}_i^\circ\right)}{\sum\limits_{n \neq i} \mathrm{Tr}\left(\mathbf{A}\mathbf{W}_n^\circ\right) + \psi_d \phi^\circ + 1} \triangleq \Xi\left(\{\mathbf{W}_n^\circ\}, \phi^\circ\right). \quad (38)$$

From (38), we can see that the maximum value of μ^* is achieved when the function $\Xi(\{\mathbf{W}_n\}_{n=1}^N, \phi)$ gets the solutions of $\{\mathbf{W}_n^\circ\}_{n=1}^N$ and ϕ°. Thus, $\{\mathbf{W}_n^\circ\}_{n=1}^N$ and ϕ° are the optimal solutions for $\mathcal{P}5$ and the proof is concluded. ■

Based on Proposition 1, $\mathcal{P}6$-A is equivalent to $\mathcal{P}7$ with a fixed ϕ. Thus, we prove the rank-one conditions in $\mathcal{P}6$-A by proving that in $\mathcal{P}7$ with the following Theorem.

Theorem 1: For any feasible ϕ, the solution of $\mathbf{W}_n$ with $n = 1, \ldots, N$ for $\mathcal{P}7$ is rank-one.

Proof: Please refer to Appendix B. ■

Based on Theorem 1, the solutions of $\mathcal{P}6$-A also hold rank-one. To sum up, it shows a tight relaxation by the SDR in the transformation from $\mathcal{P}4$ to $\mathcal{P}5$.

D. Complexity Analysis

A two-stage optimization approach is carried out to solve the problem. In the outer stage, the one-dimensional search is employed for the single variable optimization, referring to problem $\mathcal{P}4$. Recall that for each outer search, the inner-stage solutions are obtained by an iterative alternating SDP and the fractional programming algorithm. Therefore, the computation complexity is calculated by the number of iterative search multiplied by the complexity of iterative alternating algorithm. Specifically, the complexity of solving SDP can be calculated by $\mathcal{O}(max\{m, n\}^4 n^{1/2})$, where m and n are the constraint order and the dimension of equality constraints for SDP, respectively. Thus the complexity of solving $\mathcal{P}6$-A is $\mathcal{O}((2N+1)^{4.5})$. For the fractional programming in $\mathcal{P}6$-B, the worst complexity of solving the subproblem (31) is to find the solution by using (34), which is a sort problem and the complexity is given by $\mathcal{O}(|\partial\mathcal{D}|)$, where $|\partial\mathcal{D}|$ is the number of points in $\partial\mathcal{D}$ with worst value of 4. In addition, the iteration number of Dinkelbach's method can be calculated as $\mathcal{O}(log(1/\epsilon_1))$ and the complexity of one-dimension search is $\mathcal{O}(log(1/\epsilon_2))$. Thus, the total complexity is given by $\mathcal{O}(log(1/\epsilon_2)log(1/\epsilon_0)((2N+1)^{4.5} + 4\ log(1/\epsilon_1)))$.

TABLE II
SYSTEM PARAMETERS SETTING

System parameters	Numerical value
Satellite-to-ground channel parameters	
Satellite height	600 Km
Carrier frequency	2 GHz
Maximum beam gain	45 dB
3 dB angle (for all beams)	0.4°
Rain attenuation parameters	$\mu_{\zeta_{dB}}$ = -3.152, $\delta^2 = 1.6$
Air-to-ground channel parameters	
Channel power gain	-40 dB
Rician factor of legitimate user	5 dB
Rician factor of Eve	0 dB
U_d of legitimate user	10 m
U_d of Eve	100 m

VI. PERFORMANCE EVALUATIONS

In this section, to evaluate the secrecy rate performance of multi-beam satellite downlink communications, extensive numerical results are carried out. The system parameters are specifically set as follows. The height of satellite orbit is 600 Km and the maximum beam gain G_{max} is set to 45 dB. The 3 dB angles of all beams are set to $\alpha_{i,3dB} = 0.4°$. The rain attenuation parameters of downlink satellite-terrestrial channels are set to $\mu_{\zeta_{dB}} = -3.152$ and $\delta^2 = 1.6$. The carrier frequency of satellite downlink transmission is 2 GHz. The channel power gain of air-to-ground at the reference distance of 1 m is -40 dB. The horizontal distance from UAV to legitimate user and Eve is 10 m and 100 m, respectively. The Rician factors of air-to-ground channels for the legitimate user and Eve are set to 5 dB and 0 dB, respectively. The same QoS requirements are preset as Q_m for users SU_j with $j \in \{1, \ldots, N\}$ and $j \neq i$.

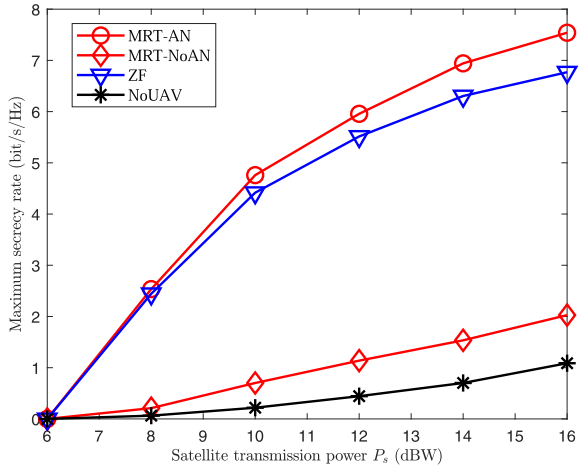

Fig. 2. Secrecy rate vs. the satellite transmission power Ps. ($P_v = 5$ dBW, $\beta = 0$ dB, $N = 4$, $M = 4$, $Q_m = 0.1$ bit/s/Hz, and $U_h = 100$ m).

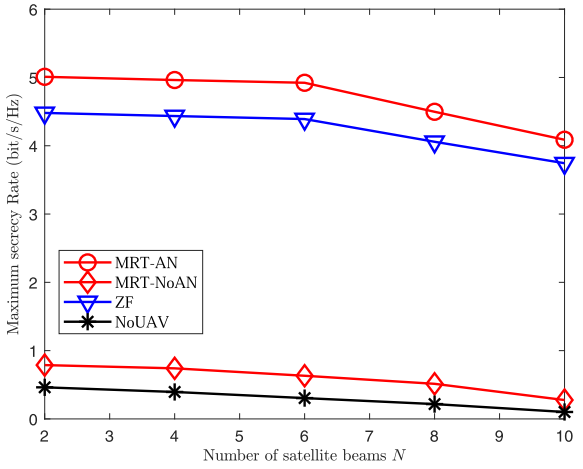

Fig. 4. Secrecy rate vs. the number of satellite beams N. ($P_s = 10$ dBW, $P_v = 5$ dBW, $\beta = 0$ dB, $M = 4$, $Q_m = 0.1$ bit/s/Hz, and $U_h = 100$ m).

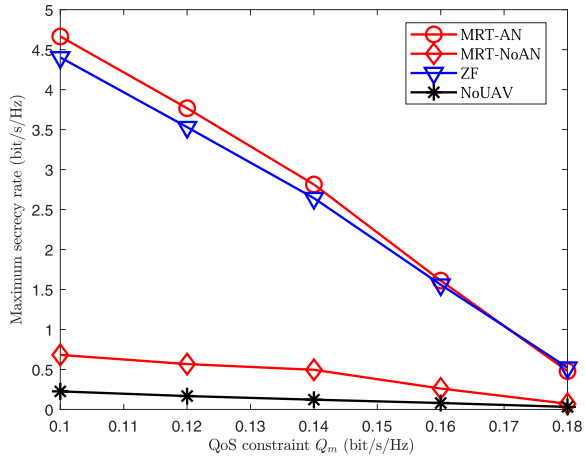

Fig. 3. Secrecy rate vs. the QoS of Q_k. ($P_s = 10$ dBW, $P_v = 5$ dBW, $\beta = 0$ dB, $N = 4$, $M = 4$, and $U_h = 100$ m).

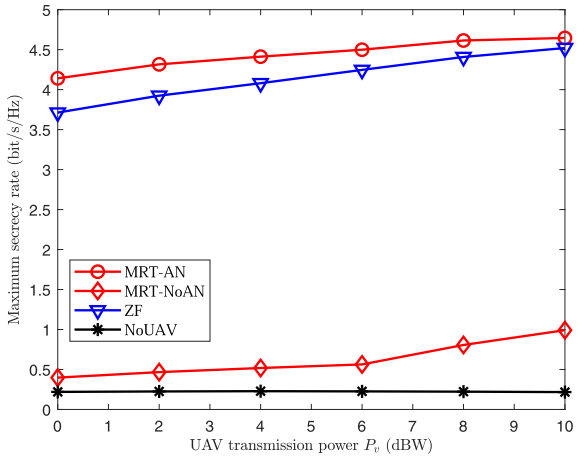

Fig. 5. Secrecy rate vs. UAV transmission power P_v. ($P_s = 10$ dBW, $\beta = 0$ dB, $N = 4$, and $M = 4$, $Q_m = 0.1$ bit/s/Hz, and $U_h = 100$ m).

Tag/Benchmark: For the proposed approach, marked by "MRT-AN", we adopt the MRT-based BF for the UAV AF link and an AN is created by UAV simultaneously. For comparisons, the "MRT-NoAN" and "ZF" approaches adopt MRT and ZF based BF for the UAV AF link, respectively, but they have no AN. In addition, the case that without UAV, marked by "NoUAV", is regarded as the benchmark, which only optimizes the satellite BF without UAV cooperation.

Fig. 2 shows the impact of satellite transmission power on the maximum secrecy rate, and we can see that the maximum secrecy rate of legitimate user is monotonically increasing of the satellite transmission power. This happens since more satellite power can be used to maximize the secrecy rate of legitimate user when the satellite power increases. In Fig. 3, we investigate the impact of QoS constraint on the maximum secrecy rate of legitimate user. It can be seen that the maximum secrecy rate decreases as the QoS constraint increases, as more satellite power should be allocated to other satellite beams to satisfy the increased QoS constraint and thus less power will be left for the legitimate user. Fig. 4 shows the impact of number of satellite beams on the maximum secrecy rate of legitimate user. It can be seen that the maximum secrecy rate decreases as the number of satellite beams increases, which happens since more satellite power is consumed to ensure the QoS constraint of co-channel users in other beams, and more co-channel interference is raised up due to the increased satellite beams.

In addition, we can observe that the MRT-AN approach outperforms ZF approach from Fig. 2 $\sim$ Fig. 4. This is because the AF signal from UAV cannot concentrate on legitimate user well by the ZF approach without degrading Eve additionally, comparing to the MRT-AN approach. By comparing two curves of MRT-AN and MRT-NoAN, it is observed that the maximum secrecy rate improves with adopting AN for the MRT-based UAV BF scheme. More specifically, with the assistance of UAV and employing our proposed approaches, the maximum secrecy rate of legitimate user is improved significantly.

In Fig. 5 $\sim$ Fig. 8, we investigate the impact of UAV parameters on the maximum secrecy rate of legitimate user,

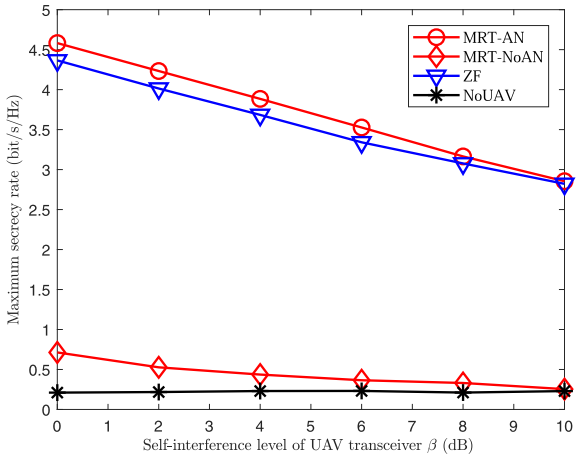

Fig. 6. Secrecy rate vs. the self-interference level of UAV transceiver β. ($P_s = 10$ dBW, $P_v = 5$ dBW, $N = 4$, $M = 4$, $Q_m = 0.1$ bit/s/Hz, and $U_h = 100$ m).

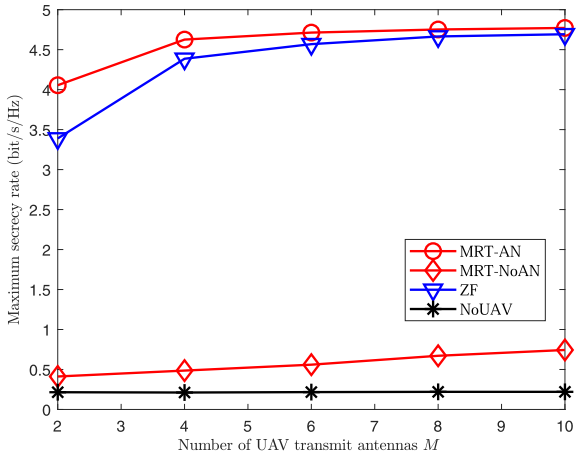

Fig. 8. Secrecy rate vs. the number of UAV transmit antennas M. ($P_s = 10$ dBW, $P_v = 5$ dBW, $\beta = 0$ dB, $N = 4$, $Q_m = 0.1$ bit/s/Hz, and $U_h = 100$ m).

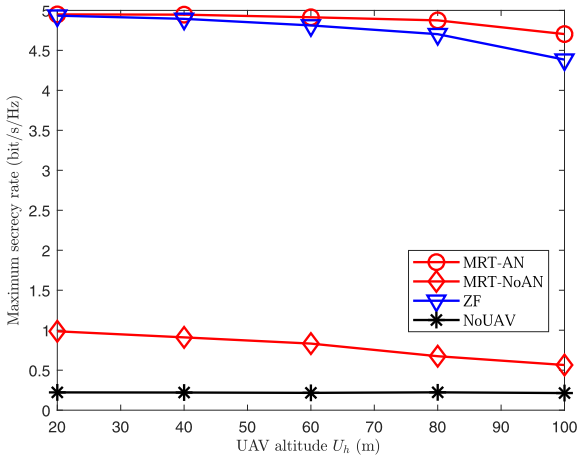

Fig. 7. Secrecy rate vs. the UAV altitude U_h. ($P_s = 10$ dBW, $P_v = 5$ dBW, $\beta = 0$ dB, $N = 4$, $M = 4$, and $Q_m = 0.1$ bit/s/Hz).

including transmission power, self-interference level of transceiver, UAV altitude, and the number of transmit antennas, respectively. In Fig. 5, it can be seen that the maximum secrecy rate increases monotonically as the UAV power increases. This happens since the signal quality of the main channel can be enhanced when the UAV power increases and more power can be leveraged to confuse Eve with AN. From Fig. 6, we can see that the maximum secrecy rate decreases as the power of self-interference increases. It is because the self-interference degrades the received SINR of legitimate user, and more degradation as the self-interference increases. In Fig. 7, it is observed that the maximum secrecy rate is monotonically decreasing of the UAV altitude. Based on (5), the channel power gain decreases as the UAV altitude increases, degrading the received SINR of legitimate user. From Fig. 8, we can see that the maximum secrecy rate increases as the number of UAV transmit antennas increases. That is because the UAV beam can focus more on its BF direction when the number of antennas increases. More specifically, when the number of UAV transmit antennas is large enough, it can be seen that the secrecy performances of MRT-AN and ZF approaches become close. This happens since the interference and leakage caused by MRT-based BF scheme and the signal loss of ZF-based scheme become negligible as the number of UAV transmit antennas increases. Particularly, the focus of AN becomes more centered on Eve, which degrades the Eve more. In addition, Fig. 5 $\sim$ Fig. 8 show that the secrecy performance of legitimate user can be enhanced by exploiting UAV, and the MRT-AN approach outperforms the ZF and MRT-NoAN approaches.

VII. Conclusion and Future Work

In this paper, we have investigated the physical layer security in multi-beam satellite-enabled vehicle communications, where the UAV has been exploited to cooperate with the legitimate user and create an AN to confuse Eve. To maximize the secrecy rate of legitimate user within the target beam while guaranteeing the QoS of users within other beams, we have formulated a problem to jointly optimize the satellite BF and UAV PA, which is then converted into an one-dimensional search problem in the outer stage and a bi-convex problem in the inner stage. For each outer-stage search, the inner-stage bi-convex problem has been solved by the devised iterative alternating optimization approach, where SDP and Dinkelbach's method have been used to alternately optimize the satellite BF and UAV PA in each iteration. Extensive simulations have been carried out and the results demonstrate that with the assistance of UAV, the secrecy rate performance can be significantly improved. For the future work, we will investigate the cross-layer security in SAGIN enabled ITSs.

Appendix A: Proof of Lemma 1

Proof: Based on (19a), the positive secrecy rate is expected, i.e., $\log_2(1+\gamma_d) - \log_2(\frac{1}{\tau}) > 0$, which requires $\frac{1}{\tau} \leq 1+\gamma_d$. Thus, we can obtain a lower bound of the slack

variable τ as follows

$$\begin{aligned}\tau &\geq \frac{1}{1+\frac{|\mathbf{a}\mathbf{w}_i|^2}{\sum\limits_{n\neq i}|\mathbf{a}\mathbf{w}_n|^2+\alpha^2\phi p_v\left|\mathbf{h}_{rd}^{\dagger}\mathbf{f}\right|^2(1+\beta)+1}}\\ &\geq \frac{1}{1+|\mathbf{a}\mathbf{w}_i|^2}\\ &= \frac{1}{1+\left|\mathbf{h}_{sd}^{\dagger}\mathbf{w}_i\right|^2+\alpha^2 P_s\left|\mathbf{h}_{rd}^{\dagger}\mathbf{f}\mathbf{h}_{sr}^{\dagger}\mathbf{w}_i\right|^2}\\ &\overset{(a)}{\geq} \frac{1}{1+P_s\left|\mathbf{h}_{sd}^{\dagger}\right|^2+\alpha^2 P_s P_v\left|\mathbf{h}_{rd}^{\dagger}\mathbf{f}\mathbf{h}_{sr}^{\dagger}\right|^2} \triangleq \tau_{\min}, \end{aligned} \tag{39}$$

where condition (a) adopts the Cauchy-Schwarz inequality. From (19b), we have $\tau \leq 1$. The proof is completed. ■

Appendix B: Proof of Theorem 1

Proof: The Lagrangian function of $\mathcal{P}7$ can be expressed as

$$\begin{aligned}&\mathcal{L}\left(\{\mathbf{W}_n, \mathbf{U}_n, n=1,\ldots,N\}, \phi, \lambda, \rho, \kappa_j, \vartheta, \varsigma_0, \varsigma_1\right)\\ &= \sum_{n=1}^{N}\mathrm{Tr}\left(\mathbf{W}_n\right) - \sum_{n=1}^{N}\mathrm{Tr}\left(\mathbf{U}_n\mathbf{W}_n\right) - \varsigma_0\phi + \varsigma_1\left(\phi-1\right)\\ &\quad - \lambda\left(\tau\mathrm{Tr}\left(\mathbf{A}\mathbf{W}_i\right) - u^*\left(\sum_{n\neq i}\mathrm{Tr}\left(\mathbf{A}\mathbf{W}_n\right)+\psi_d\phi\right) - u^*\right)\\ &\quad + \rho\left(\mathrm{Tr}\left(\mathbf{B}\mathbf{W}_{\Delta}\right) - \xi p_v\mathrm{Tr}\left(\mathbf{H}_{re}\mathbf{C}\right) - \xi\psi_e\phi - \xi\right)\\ &\quad - \sum_{j\neq i}\kappa_j\left(\mathrm{Tr}\left(\mathbf{H}_j\left(\mathbf{W}_j - \sum_{n\neq j}\varepsilon_j\mathbf{W}_n\right)\right) - \varepsilon_j\right)\\ &\quad + \vartheta\left(\sum_{n=1}^{N}\mathrm{Tr}\left(\mathbf{W}_n\right) - P_s\right), \end{aligned} \tag{40}$$

where $\lambda \geq 0$, $\{\kappa_j\} \geq 0$, $\rho \geq 0$, $\mathbf{U}_n \succeq \mathbf{0}$, $\varsigma_0 \geq 0$, and $\varsigma_1 \geq 0$.

To prove the rank condition of $\mathbf{W}_i$, Karush-Kuhn-Tucker (KKT) conditions are adopted. Based on (40), we take the partial derivative of the Lagrangian function with respect to $\mathbf{W}_i$ and apply KKT conditions, we have

$$\left(1+\vartheta\right)\mathbf{I}_N + \rho\mathbf{B} + \sum_{j\neq i}\kappa_j\mathbf{H}_j\varepsilon_j - \lambda\tau\mathbf{A} - \mathbf{U}_i = \mathbf{0}, \tag{41}$$

$$\mathbf{U}_i\mathbf{W}_i = \mathbf{0}, \tag{42}$$

$$\mathbf{W}_i \succeq \mathbf{0}. \tag{43}$$

By post-multiplying both sides of (41) with $\mathbf{W}_i$ and using (42), (41) can be written as

$$\left(\left(1+\vartheta\right)\mathbf{I}_N + \rho\mathbf{B} + \sum_{j\neq i}\kappa_j\mathbf{H}_j\varepsilon_j\right)\mathbf{W}_i = \lambda\tau\mathbf{A}\mathbf{W}_i. \tag{44}$$

In (44), it is observed that

$$\left(1+\vartheta\right)\mathbf{I}_N + \rho\mathbf{B} + \sum_{j\neq i}\kappa_j\mathbf{H}_j\varepsilon_j \succ \mathbf{0}, \tag{45}$$

since $\vartheta \geq 0, \rho \geq 0$, and $\{\kappa_j\} \geq 0$. In addition, we have $\mathrm{Rank}\left(\mathbf{A}\right) = 1$ due to $\mathbf{A} = \mathbf{a}^{\dagger}\mathbf{a}$. Thus,

$$\mathrm{Rank}(\mathbf{W}_i) = \mathrm{Rank}(\mathbf{A}\mathbf{W}_i) \leq \mathrm{Rank}(\lambda\tau\mathbf{A}) = 1, \tag{46}$$

where $\lambda\tau > 0$.[4] Discarding a trivial case of $\mathbf{W}_i = \mathbf{0}$, $\mathrm{Rank}(\mathbf{W}_i) = 1$ is proved. Next, we prove the rank condition of $\mathbf{W}_j$ $(j \neq i)$.

Based on (40), we take the partial derivative of the Lagrangian function with respect to $\mathbf{W}_j (j \neq i)$, and apply KKT conditions, we have

$$\mathbf{D} - \kappa_j\mathbf{H}_j - \rho\xi\mathbf{B} - \mathbf{U}_j = \mathbf{0}, \tag{47}$$

$$\mathbf{U}_j\mathbf{W}_j = \mathbf{0}, \tag{48}$$

$$\mathbf{W}_j \succeq \mathbf{0}, \tag{49}$$

where $\mathbf{D} = \left(1+\vartheta\right)\mathbf{I}_N + \lambda u^*\mathbf{A} + \sum\limits_{\ell\neq j,\ell\neq i}\kappa_\ell\varepsilon_\ell\mathbf{H}_\ell$ with full rank, since $\vartheta \geq 0, \lambda \geq 0, u^* > 0$, and $\{\kappa_\ell\} \geq 0$. Further, by denoting $\mathbf{E} = \mathbf{D} - \kappa_j\mathbf{H}_j$, we have

$$N - 1 \leq \mathrm{Rank}\left(\mathbf{E}\right) \leq N. \tag{50}$$

Based on (47) and (50), and denoting $\mathbf{Z} = \rho\xi\mathbf{B} + \mathbf{U}_j$, we have $\mathrm{Rank}\left(\mathbf{Z}\right) \geq N - 1$.

On the other hand, using the Sylvester inequality, we can obtain

$$\mathrm{Rank}\left(\mathbf{Z}\right) + \mathrm{Rank}\left(\mathbf{W}_j\right) \leq \mathrm{Rank}\left(\mathbf{Z}\mathbf{W}_j\right) + N, \tag{51}$$

where $\mathrm{Rank}\left(\mathbf{Z}\mathbf{W}_j\right)$ satisfies

$$\mathrm{Rank}\left(\mathbf{Z}\mathbf{W}_j\right) = \mathrm{Rank}\left(\rho\xi\mathbf{B}\mathbf{W}_j\right) \leq \mathrm{Rank}\left(\mathbf{B}\right) = 1, \tag{52}$$

due to $\mathbf{B} = \mathbf{b}^{\dagger}\mathbf{b}$. From (52), if $\mathrm{Rank}\left(\rho\xi\mathbf{B}\mathbf{W}_j\right) = 1$, which indicates the condition $\mathrm{Rank}\left(\mathbf{W}_i\right) = N$ should be satisfied and thus $\mathrm{Rank}\left(\mathbf{Z}\mathbf{W}_j\right) = 1$ is achieved. Therefore, the condition in (51) becomes

$$\mathrm{Rank}\left(\mathbf{Z}\right) + \mathrm{Rank}\left(\mathbf{W}_j\right) \leq N + 1, \tag{53}$$

where $\mathrm{Rank}\left(\mathbf{Z}\right) \leq 1$ is reached. However, it is conflict with the previously proven $\mathrm{Rank}\left(\mathbf{Z}\right) \geq N - 1$. Therefore, the only provision of $\mathrm{Rank}\left(\mathbf{Z}\mathbf{W}_j\right) = 0$ is satisfied. Return to (51), we have

$$\mathrm{Rank}\left(\mathbf{Z}\right) + \mathrm{Rank}\left(\mathbf{W}_j\right) \leq N, \tag{54}$$

which indicates that $\mathrm{Rank}\left(\mathbf{W}_j\right) \leq 1$ due to $\mathrm{Rank}\left(\mathbf{Z}\right) \geq N-1$. Since the positive secrecy rate, $\mathbf{W}_j = \mathbf{0}$ cannot be a solution, thus $\mathrm{Rank}\left(\mathbf{W}_j\right) = 1$. The proof is completed. ■

References

[1] S. Zhou, G. Wang, S. Zhang, Z. Niu, and X. S. Shen, "Bidirectional mission offloading for agile space-air-ground integrated networks," *IEEE Wireless Commun.*, vol. 26, no. 2, pp. 38–45, Apr. 2019.

[2] X. Cheng *et al.*, "Space/aerial-assisted computing offloading for IoT applications: A learning-based approach," *IEEE J. Sel. Areas Commun.*, vol. 37, no. 5, pp. 1117–1129, May 2019.

[3] N. Zhang, S. Zhang, P. Yang, O. Alhussein, W. Zhuang, and X. S. Shen, "Software defined space-air-ground integrated vehicular networks: Challenges and solutions," *IEEE Commun. Mag.*, vol. 55, no. 7, pp. 101–109, Jul. 2017.

[4] F. Lyu *et al.*, "Characterizing urban vehicle-to-vehicle communications for reliable safety applications," *IEEE Trans. Intell. Transp. Syst.*, vol. 21, no. 6, pp. 2586–2602, Jun. 2020.

[5] X. Han *et al.*, "Reliability-aware joint optimization for cooperative vehicular communication and computing," *IEEE Trans. Intell. Transp. Syst.*, early access, Dec. 14, 2021, doi: 10.1109/TITS.2020.3038558.

[4] It is easy to prove that $\mathbf{W}_i = \mathbf{0}$ if $\lambda\tau = 0$, which should be discarded.

[6] W. Shi, H. Zhou, J. Li, W. Xu, N. Zhang, and X. Shen, "Drone assisted vehicular networks: Architecture, challenges and opportunities," *IEEE Netw.*, vol. 32, no. 3, pp. 130–137, May 2018.

[7] Y. Cao, T. Jiang, O. Kaiwartya, H. Sun, H. Zhou, and R. Wang, "Toward pre-empted EV charging recommendation through V2V-based reservation system," *IEEE Trans. Syst., Man, Cybern., Syst.*, vol. 51, no. 5, pp. 3026–3039, May 2021.

[8] Y. Cao and N. Wang, "Toward efficient electric-vehicle charging using VANET-based information dissemination," *IEEE Trans. Veh. Technol.*, vol. 66, no. 4, pp. 2886–2901, Apr. 2017.

[9] B. Li, Z. Fei, C. Zhou, and Y. Zhang, "Physical-layer security in space information networks: A survey," *IEEE Internet Things J.*, vol. 7, no. 1, pp. 33–52, Jan. 2020.

[10] C. Zhao, M. Shi, M. Huang, and X. Du, "Authentication scheme based on Hashchain for space-air-ground integrated network," in *Proc. IEEE Int. Conf. Commun. (ICC)*, May 2019, pp. 1–6.

[11] X. Luo, Y. Liu, H.-H. Chen, and Q. Guo, "Physical layer security in intelligently connected vehicle networks," *IEEE Netw.*, vol. 34, no. 5, pp. 232–239, Sep. 2020.

[12] W. Wang, K. C. Teh, S. Luo, and K. H. Li, "Physical layer security in heterogeneous networks with pilot attack: A stochastic geometry approach," *IEEE Trans. Commun.*, vol. 66, no. 12, pp. 6437–6449, Dec. 2018.

[13] R. Zhao, H. Lin, Y.-C. He, D.-H. Chen, Y. Huang, and L. Yang, "Secrecy performance of transmit antenna selection for MIMO relay systems with outdated CSI," *IEEE Trans. Commun.*, vol. 66, no. 2, pp. 546–559, Feb. 2018.

[14] Y. Liu, H.-H. Chen, L. Wang, and W. Meng, "Artificial noisy MIMO systems under correlated scattering Rayleigh fading—A physical layer security approach," *IEEE Syst. J.*, vol. 14, no. 2, pp. 2121–2132, Jun. 2020.

[15] B. Li, Z. Fei, Z. Chu, F. Zhou, K.-K. Wong, and P. Xiao, "Robust chance-constrained secure transmission for cognitive satellite–terrestrial networks," *IEEE Trans. Veh. Technol.*, vol. 67, no. 5, pp. 4208–4219, May 2018.

[16] M. Lin, Z. Lin, W.-P. Zhu, and J.-B. Wang, "Joint beamforming for secure communication in cognitive satellite terrestrial networks," *IEEE J. Sel. Areas Commun.*, vol. 36, no. 5, pp. 1017–1029, May 2018.

[17] J. Du, C. Jiang, H. Zhang, X. Wang, Y. Ren, and M. Debbah, "Secure satellite-terrestrial transmission over incumbent terrestrial networks via cooperative beamforming," *IEEE J. Sel. Areas Commun.*, vol. 36, no. 7, pp. 1367–1382, Jul. 2018.

[18] Z. Lin, M. Lin, J. Ouyang, W.-P. Zhu, A. D. Panagopoulos, and M.-S. Alouini, "Robust secure beamforming for multibeam satellite communication systems," *IEEE Trans. Veh. Technol.*, vol. 68, no. 6, pp. 6202–6206, Jun. 2019.

[19] P. K. Sharma and D. I. Kim, "Secure 3D mobile UAV relaying for hybrid satellite-terrestrial networks," *IEEE Trans. Wireless Commun.*, vol. 19, no. 4, pp. 2770–2784, Apr. 2020.

[20] Z. Yin *et al.*, "Secrecy rate analysis of satellite communications with frequency domain NOMA," *IEEE Trans. Veh. Technol.*, vol. 68, no. 12, pp. 11847–11858, Dec. 2019.

[21] K. An, M. Lin, J. Ouyang, and W.-P. Zhu, "Secure transmission in cognitive satellite terrestrial networks," *IEEE J. Sel. Areas Commun.*, vol. 34, no. 11, pp. 3025–3037, Nov. 2016.

[22] S. K. Sharma, S. Chatzinotas, and B. Ottersten, "Cognitive beamhopping for spectral coexistence of multibeam satellites," *Int. J. Satell. Commun. Netw.*, vol. 33, no. 1, pp. 69–91, Mar. 2014.

[23] M. A. Vazquez *et al.*, "Precoding, scheduling, and link adaptation in mobile interactive multibeam satellite systems," *IEEE J. Sel. Areas Commun.*, vol. 36, no. 5, pp. 971–980, May 2018.

[24] G. Colavolpe, A. Modenini, A. Piemontese, and A. Ugolini, "Multi-user detection in multibeam satellite systems: Theoretical analysis and practical schemes," *IEEE Trans. Commun.*, vol. 65, no. 2, pp. 945–955, Feb. 2017.

[25] G. Zheng, P.-D. Arapoglou, and B. Ottersten, "Physical layer security in multibeam satellite systems," *IEEE Trans. Wireless Commun.*, vol. 11, no. 2, pp. 852–863, Feb. 2012.

[26] V. Joroughi, M. A. Vazquez, and A. I. Perez-Neira, "Generalized multicast multibeam precoding for satellite communications," *IEEE Trans. Wireless Commun.*, vol. 16, no. 2, pp. 952–966, Feb. 2017.

[27] R. T. Schwarz, T. Delamotte, K.-U. Storek, and A. Knopp, "MIMO applications for multibeam satellites," *IEEE Trans. Broadcast.*, vol. 65, no. 4, pp. 664–681, Dec. 2019.

[28] C. Masouros and G. Zheng, "Exploiting known interference as green signal power for downlink beamforming optimization," *IEEE Trans. Signal Process.*, vol. 63, no. 14, pp. 3628–3640, Jul. 2015.

[29] P. Series, *Propagation Data and Prediction Methods Required for the Design of Earth-Space Telecommunication Systems*, document Recommendation ITU-R, 2015, pp. 612–618.

[30] W. Shi *et al.*, "Multi-drone 3-D trajectory planning and scheduling in drone-assisted radio access networks," *IEEE Trans. Veh. Technol.*, vol. 68, no. 8, pp. 8145–8158, Aug. 2019.

[31] Q. Song, F.-C. Zheng, Y. Zeng, and J. Zhang, "Joint beamforming and power allocation for UAV-enabled full-duplex relay," *IEEE Trans. Veh. Technol.*, vol. 68, no. 2, pp. 1657–1671, Feb. 2019.

[32] B. Duo, Q. Wu, X. Yuan, and R. Zhang, "Energy efficiency maximization for full-duplex UAV secrecy communication," *IEEE Trans. Veh. Technol.*, vol. 69, no. 4, pp. 4590–4595, Apr. 2020.

[33] L. J. Rodriguez, N. H. Tran, and T. Le-Ngoc, "Performance of full-duplex AF relaying in the presence of residual self-interference," *IEEE J. Sel. Areas Commun.*, vol. 32, no. 9, pp. 1752–1764, Sep. 2014.

[34] L. Lv, Z. Ding, Q. Ni, and J. Chen, "Secure MISO-NOMA transmission with artificial noise," *IEEE Trans. Veh. Technol.*, vol. 67, no. 7, pp. 6700–6705, Jul. 2018.

[35] P. K. Upadhyay and P. K. Sharma, "Max-max user-relay selection scheme in multiuser and multirelay hybrid satellite-terrestrial relay systems," *IEEE Commun. Lett.*, vol. 20, no. 2, pp. 268–271, Feb. 2016.

[36] Q. Li, Y. Yang, W.-K. Ma, M. Lin, J. Ge, and J. Lin, "Robust cooperative beamforming and artificial noise design for physical-layer secrecy in AF multi-antenna multi-relay networks," *IEEE Trans. Signal Process.*, vol. 63, no. 1, pp. 206–220, Jan. 2015.

[37] M. Grant and S. Boyd. (2014). *CVX: MATLAB Software for Disciplined Convex Programming, Version 2.1*. [Online]. Available: http://cvxr.com/cvx

[38] D. W. K. Ng, E. S. Lo, and R. Schober, "Energy-efficient resource allocation for secure OFDMA systems," *IEEE Trans. Veh. Technol.*, vol. 61, no. 6, pp. 2572–2585, Jul. 2012.

[39] S. Schaible, "Fractional programming. II, on Dinkelbach's algorithm," *Manage. Sci.*, vol. 22, no. 8, pp. 868–873, Apr. 1976.

Zhisheng Yin (Member, IEEE) received the B.E. degree from the Wuhan Institute of Technology, Wuhan, China, the B.B.A. degree from the Zhongnan University of Economics and Law, Wuhan, in 2012, the M.Sc. degree from the Civil Aviation University of China, Tianjin, China, in 2016, and the Ph.D. degree from the School of Electronics and Information Engineering, Harbin Institute of Technology, Harbin, China, in 2020. From September 2018 to September 2019, he visited with the BBCR Group, Department of Electrical and Computer Engineering, University of Waterloo, Canada. He is currently an Assistant Professor with the School of Cyber Engineering, Xidian University, Xi'an, China. His research interests include space-air-ground integrated networks, wireless communications, cybertwin, and physical layer security.

Min Jia (Senior Member, IEEE) received the dual Ph.D. degree from Sung Kyung Kwan University, Seoul, South Korea, and the Harbin Institute of Technology, Harbin, China, in 2010. She is currently a Professor and a Ph.D. Supervisor with the Communication Research Center, School of Electronics and Information Engineering, Harbin Institute of Technology. Her current research interests include cognitive radio, digital signal processing, machine learning, and broadband satellite communications.

Nan Cheng (Member, IEEE) received the B.E. and M.S. degrees from the Department of Electronics and Information Engineering, Tongji University, Shanghai, China, in 2009 and 2012, respectively, and the Ph.D. degree from the Department of Electrical and Computer Engineering, University of Waterloo, in 2016. He worked as a Post-Doctoral Fellow with the Department of Electrical and Computer Engineering, University of Toronto, from 2017 to 2019. He is currently a Professor with the State Key Laboratory of ISN, School of Telecommunication Engineering, Xidian University, Xi'an, China. His current research areas focus on B5G/6G, space-air-ground integrated networks, big data in vehicular networks, self-driving systems, performance analysis, MAC, opportunistic communication, and application of AI for vehicular networks.

Wei Wang (Member, IEEE) received the B.Eng. degree in information countermeasure technology and the M.Eng. degree in signal and information processing from Xidian University, Xi'an, China, in 2011 and 2014, respectively, and the Ph.D. degree in electrical and electronic engineering from Nanyang Technological University (NTU) in 2018. He worked as a Post-Doctoral Fellow with the Department of Electrical and Computer Engineering, University of Waterloo, Canada, from September 2018 to September 2019. His research interests include wireless communications, space-air-ground integrated networks, wireless security, and physical layer security. He received the IEEE Student Travel Grants for IEEE ICC'17 and the Chinese Government Award for Outstanding Self-Financed Students Abroad in 2019.

Feng Lyu (Member, IEEE) received the B.S. degree in software engineering from Central South University, Changsha, China, in 2013, and the Ph.D. degree from the Department of Computer Science and Engineering, Shanghai Jiao Tong University, Shanghai, China, in 2018. From September 2018 to December 2019 and October 2016 to October 2017, he worked as a Post-Doctoral Fellow and a Visiting Ph.D. Student with the BBCR Group, Department of Electrical and Computer Engineering, University of Waterloo, Canada. He is currently a Professor with the School of Computer Science and Engineering, Central South University, Changsha, China. His research interests include vehicular networks, beyond 5G networks, big data measurement and application design, and could/edge computing. He served as a TPC member for many international conferences. He is a member of the IEEE Computer Society, Communication Society, and Vehicular Technology Society. He was a recipient of the Best Paper Award of IEEE ICC 2019 and Norbert Wiener Review Award 2020 of IEEE/CAA JOURNAL OF AUTOMATICA SINICA. He currently serves as an Associate Editor for IEEE SYSTEMS JOURNAL, a Leading Guest Editor for *Peer-to-Peer Networking and Applications*, and a Guest Editor for *China Communications*.

Qing Guo (Member, IEEE) received the M.Eng. and Ph.D. degrees in information and communication engineering from the Harbin Institute of Technology, Harbin, China, in 1990 and 1998, respectively. He is currently a Professor and the Dean with the School of Electronics and Information Engineering, Harbin Institute of Technology. His research interests include satellite communications, deep space communications, wireless transmission, and broadband multimedia communication techniques.

Xuemin (Sherman) Shen (Fellow, IEEE) received the Ph.D. degree in electrical engineering from Rutgers University, New Brunswick, NJ, USA, in 1990.

He is a University Professor with the Department of Electrical and Computer Engineering, University of Waterloo, Canada. His research focuses on network resource management, wireless network security, the Internet of Things, 5G and beyond, and vehicular *ad hoc*, and sensor networks.

Dr. Shen is a registered Professional Engineer in Canada, an Engineering Institute of Canada Fellow, a Canadian Academy of Engineering Fellow, a Royal Society of Canada Fellow, a Chinese Academy of Engineering Foreign Member, and a Distinguished Lecturer of the IEEE Vehicular Technology Society and Communications Society. He received the Canadian Award for Telecommunications Research from the Canadian Society of Information Theory (CSIT) in 2021; the R. A. Fessenden Award from IEEE in 2019, Canada; the Award of Merit from the Federation of Chinese Canadian Professionals, ON, Canada, in 2019; the James Evans Avant Garde Award from the IEEE Vehicular Technology Society in 2018; the Joseph LoCicero Award in 2015 and Education Award in 2017 from the IEEE Communications Society; and the Technical Recognition Award from Wireless Communications Technical Committee in 2019 and AHSN Technical Committee in 2013. He has also received the Excellent Graduate Supervision Award from the University of Waterloo in 2006 and the Premier's Research Excellence Award (PREA) from the Province of Ontario, Canada, in 2003. He served as the Technical Program Committee Chair/Co-Chair for IEEE Globecom'16, IEEE Infocom'14, IEEE VTC'10 Fall, and IEEE Globecom'07; and the Chair for the IEEE Communications Society Technical Committee on Wireless Communications. He is the President Elect of the IEEE Communications Society. He was the Vice President for Technical and Educational Activities, the Vice President for Publications, a Member-at-Large on the Board of Governors, the Chair of the Distinguished Lecturer Selection Committee, and a member of IEEE Fellow Selection Committee of the ComSoc. He served as the Editor-in-Chief of the IEEE INTERNET OF THINGS JOURNAL (IoT), *IEEE Network*, and *IET Communications*.